World Journal of Gastroenterology

Submit a Manuscript: http://www.f6publishing.com

World J Gastroenterol 2018 September 7; 24(33): 3786-3798

DOI: 10.3748/wjg.v24.i33.3786

ISSN 1007-9327 (print) ISSN 2219-2840 (online)

ORIGINAL ARTICLE

Retrospective Study

Differentiation of intrahepatic cholangiocarcinoma from hepatocellular carcinoma in high-risk patients: A predictive model using contrast-enhanced ultrasound

Li-Da Chen, Si-Min Ruan, Jin-Yu Liang, Zheng Yang, Shun-Li Shen, Yang Huang, Wei Li, Zhu Wang, Xiao-Yan Xie, Ming-De Lu, Ming Kuang, Wei Wang

Li-Da Chen, Si-Min Ruan, Jin-Yu Liang, Yang Huang, Wei Li, Zhu Wang, Xiao-Yan Xie, Ming-De Lu, Ming Kuang, Wei Wang, Department of Medical Ultrasonics, Institute of Diagnostic and Interventional Ultrasound, The First Affiliated Hospital of Sun Yat-Sen University, Guangzhou 510080, Guangdong Province, China

Zheng Yang, Department of Pathology, The Seventh Affiliated Hospital of Sun Yat-Sen University, Guangzhou 510080, Guangdong Province, China

Shun-Li Shen, Ming-De Lu, Ming Kuang, Department of Hepatobiliary Surgery, The First Affiliated Hospital of Sun Yat-Sen University, Guangzhou 510080, Guangdong Province, China

ORCID number: Li-Da Chen (0000-0001-9904-2195); Si-Min Ruan (0000-0002-1121-3664); Jin-Yu Liang (0000-0002-1121-3664); Zheng Yang (0000-0002-1121-3664); Shun-Li Shen (0000-0002-1121-3664); Yang Huang (0000-0002-1121-3664); Wei Li (0000-0002-1121-3664); Zhu Wang (0000-0002-4272-3501); Xiao-Yan Xie (0000-0002-4272-3501); Ming-De Lu (0000-0002-4272-3501); Ming Kuang (0000-0002-7397-5779); Wei Wang (0000-0002-9485-583X).

Author contributions: Chen LD, Ruan SM, Wang W, Xie XY, Lu MD, Kuang M designed the research; Chen LD, Ruan SM, Wang W, Liang JY, Huang Y performed the research; Chen LD and Ruan SM contributed equally to the design and preparation of this study and should be considered co-first authors; Li W, Wang Z contributed new reagents or analytical tools; Yang Z, Shen SL analyzed data; Chen LD, Ruan SM wrote the paper.

Supported by the National Nature Science Foundation of China, No. 81701719; the Guangdong Science and Technology Foundation, No. 2017A020215195; and the Guangdong Medical Scientific Research Foundation, No. A2016254.

Institutional review board statement: This study was approved by the Institutional Review Board of the First Affiliated Hospital of Sun Yat-Sen University.

Informed consent statement: Informed consent was obtained from each patient.

Conflict-of-interest statement: The authors have declared no conflicts of interest.

Manuscript source: Unsolicited manuscript

Correspondence to: Wei Wang, MD, PhD, Associate Professor, Department of Medical Ultrasonics, Institute of Diagnostic and Interventional Ultrasound, The First Affiliated Hospital of Sun Yat-Sen University, 58 Zhongshan Road 2, Guangzhou 510080, Guangdong Province, China. wangw73@mail.sysu.edu.cn
Telephone: +86-20-87765183
Fax: +86-20-87765183

Received: May 7, 2018
Peer-review started: May 7, 2018
First decision: May 16, 2018
Revised: June 30, 2018
Accepted: July 16, 2018
Article in press: July 16, 2018
Published online: September 7, 2018

Abstract

AIM

To develop a contrast-enhanced ultrasound (CEUS)

predictive model for distinguishing intrahepatic cholangiocarcinoma (ICC) from hepatocellular carcinoma (HCC) in high-risk patients.

METHODS

This retrospective study consisted of 88 consecutive high-risk patients with ICC and 88 high-risk patients with HCC selected by propensity score matching between May 2004 and July 2016. Patients were assigned to two groups, namely, a training set and validation set, at a 1:1 ratio. A CEUS score for diagnosing ICC was generated based on significant CEUS features. Then, a nomogram based on the CEUS score was developed, integrating the clinical data. The performance of the nomogram was then validated and compared with that of the LR-M of the CEUS Liver Imaging Reporting and Data System (LI-RADS).

RESULTS

The most useful CEUS features for ICC were as follows: rim enhancement (64.5%), early washout (91.9%), intratumoral vein (58.1%), obscure boundary of intratumoral non-enhanced area (64.5%), and marked washout (61.3%, all $P < 0.05$). In the validation set, the area under the curve (AUC) of the CEUS score (AUC = 0.953) for differentiation between ICC and HCC was improved compared to the LI-RADS (AUC = 0.742) ($P < 0.001$). When clinical data were added, the CEUS score nomogram was superior to the LI-RADS nomogram (AUC: 0.973 *vs* 0.916, $P = 0.036$, Net Reclassification Improvement: 0.077, Integrated Discrimination Index: 0.152). Subgroup analysis demonstrated that the CEUS score model was notably improved compared to the LI-RADS in tumors smaller than 5.0 cm ($P < 0.05$) but not improved in tumors smaller than 3.0 cm ($P > 0.05$).

CONCLUSION

The CEUS predictive model for differentiation between ICC and HCC in high-risk patients had improved discrimination and clinical usefulness compared to the CEUS LI-RADS.

Key words: Ultrasonography; Hepatocellular carcinoma; Intrahepatic cholangiocarcinoma; Hepatitis

Core tip: A contrast-enhanced ultrasound (CEUS) score for predicting intrahepatic cholangiocarcinoma (ICC) consisting of more detailed CEUS features was constructed. The diagnostic performance of the CEUS score for differentiation between ICC and hepatocellular carcinoma were improved compared to the LR-M of the Liver Imaging Reporting and Data System (LI-RADS). A CEUS score nomogram, which added the clinical risk factors, was superior to the LI-RADS nomogram.

Chen LD, Ruan SM, Liang JY, Yang Z, Shen SL, Huang Y, Li W, Wang Z, Xie XY, Lu MD, Kuang M, Wang W. Differentiation of intrahepatic cholangiocarcinoma from hepatocellular carcinoma in high-risk patients: A predictive model using contrast-enhanced ultrasound. *World J Gastroenterol* 2018; 24(33): 3786-3798 Available from: URL: http://www.wjgnet.com/1007-9327/full/v24/i33/3786.htm DOI: http://dx.doi.org/10.3748/wjg.v24.i33.3786

INTRODUCTION

Intrahepatic cholangiocarcinoma (ICC) is a highly malignant epithelial cancer originating from bile ducts with cholangiocyte differentiation[1]. In recent years, chronic cirrhosis and viral hepatitis have been recognized as important risk factors for ICC development[2]. ICC has been increasingly found in patients with cirrhosis[3], and distinguishing between ICC and hepatocellular carcinoma (HCC) is a major clinical issue because the management and prognosis of these conditions differ significantly[4].

In recent years, the value of contrast-enhanced ultrasound (CEUS) for distinguishing ICC from HCC has been controversial. Vilana *et al*[5] has pointed out that ICC in cirrhosis shares a similar enhancement pattern to that of HCC on CEUS (47.6%, 10/21), which may lead to a false-positive diagnosis of HCC. Therefore, CEUS has been eliminated from the HCC diagnostic flowchart in the updated American Association for the Study of Liver Diseases (AASLD) 2011 guidelines[6]. This removal has caused controversy and has not been widely accepted in Europe or Asia[7-10] because the study by Vilana R was only based on a rather small sample size without differential diagnostic analysis of ICC versus HCC.

In 2016, the American College of Radiology (ACR) released the CEUS Liver Imaging Reporting and Data System® (LI-RADS®). The CEUS LI-RADS® standardizes the CEUS diagnostic system for patients at risk for developing HCC. In this system, the diagnosis of HCC should be distinguished from that of not only benign lesions (LR-1 or LR-2) but also other malignancies of the liver, namely, LR-M. LR-M represents a category for lesions that are definitely or probably malignant, and their features are defined as rim enhancement and early and/or marked washout. These features most closely refer to the appearance of ICC. The CEUS LI-RADS® sets the specific category of LR-M for distinguishing ICC from HCC, but the diagnostic dilemma remains unresolved. Additionally, no study has validated the performance of LR-M as the differential diagnostic criterion for ICC and HCC.

Since our first study in 2010, several studies have assessed the usefulness of CEUS in the differentiation of ICC and HCC[11-17]. Because ICCs are rare in cirrhotic livers[17], only two of these studies were able to test the performance of differential diagnosis from HCC in high-risk patients[15,16]. Several reports indicated that the typical rim-like hyperenhancement of ICC,

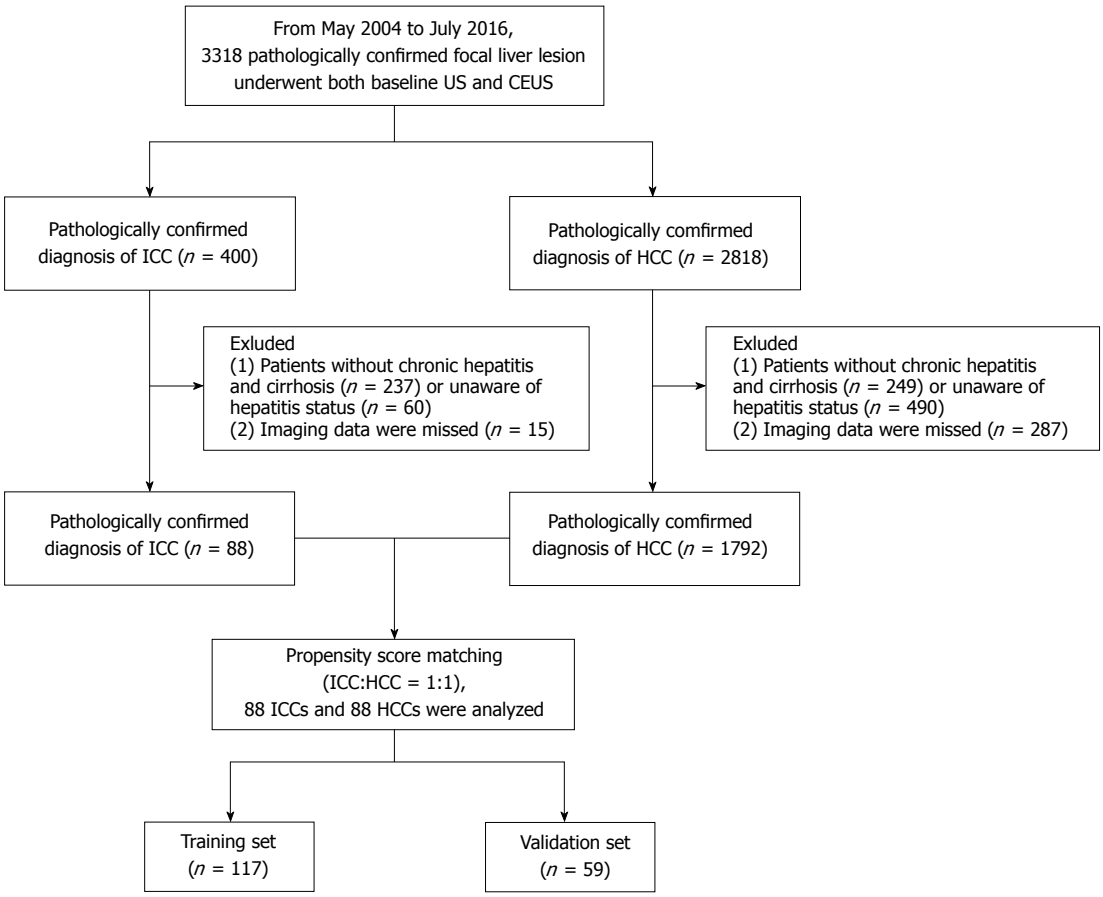

Figure 1 Flowchart of the intrahepatic cholangiocarcinoma and hepatocellular carcinoma patient selection process. CEUS: Contrast-enhanced ultrasound; HCC: Hepatocellular carcinoma; ICC: Intrahepatic cholangiocarcinoma.

recommended by the EFSUMB guideline, was observed in 8.0% to 69.2% of high-risk patients[16,18-20]. The time point for early washout was also defined within 40 s, 43 s or 60 s after contrast agent injection in three different cohorts[14-16]. Unfortunately, the differentiation criteria based on the above features varied greatly, with the sensitivity ranging from 64.1% to 87.9% and the specificity ranging from 17.9% to 97.4%[15,16]. The inconsistency indicated that ICCs in high-risk patients required further investigation from real-time CEUS, especially in comparative studies with HCC using a larger sample size.

In light of the abovementioned issues, we sought to identify important imaging predictors of ICC on CEUS, to develop a novel diagnostic nomogram incorporating clinical, CEUS and laboratory characteristics that could be used to accurately predict the risk of ICC in high-risk patients and to compare the nomogram with modified CEUS LI-RADS.

MATERIALS AND METHODS

Patients

This study was approved by the institutional review board, and informed consent was obtained from each patient. From May 2004 to July 2016, we enrolled 400 consecutive patients with ICC and 2818 consecutive patients with HCC who underwent both baseline ultrasound (US) and CEUS.

The inclusion criteria were (1) a pathologically confirmed diagnosis of ICC or HCC and (2) high-risk patients comprising patients with chronic hepatitis B and/or hepatitis C infection confirmed *via* laboratory tests[21] and cirrhosis of any cause confirmed by pathological examination via liver biopsy or surgery.

The exclusion criteria included (1) mixed hepatocellular cholangiocarcinoma (n = 45) or (2) missing imaging data (n = 302). Finally, 88 patients with ICC and 1792 patients with HCC were included at baseline (to match for the propensity score).

Propensity score matching was used to reduce the effect of selection bias in retrospective observational studies[22]. The variables for matching were tumor size and number of nodules. ICC and HCC patients were then matched 1:1 using a three-digit matching algorithm with the nearest modality.

The selection flow diagram for the study population is presented in Figure 1.

Basic clinical data, including age and sex, were recorded. Laboratory tests included hepatitis status, alpha-fetoprotein (AFP) levels, and CA 19-9 levels.

Histopathological standard

Histopathological examination was the reference stan-

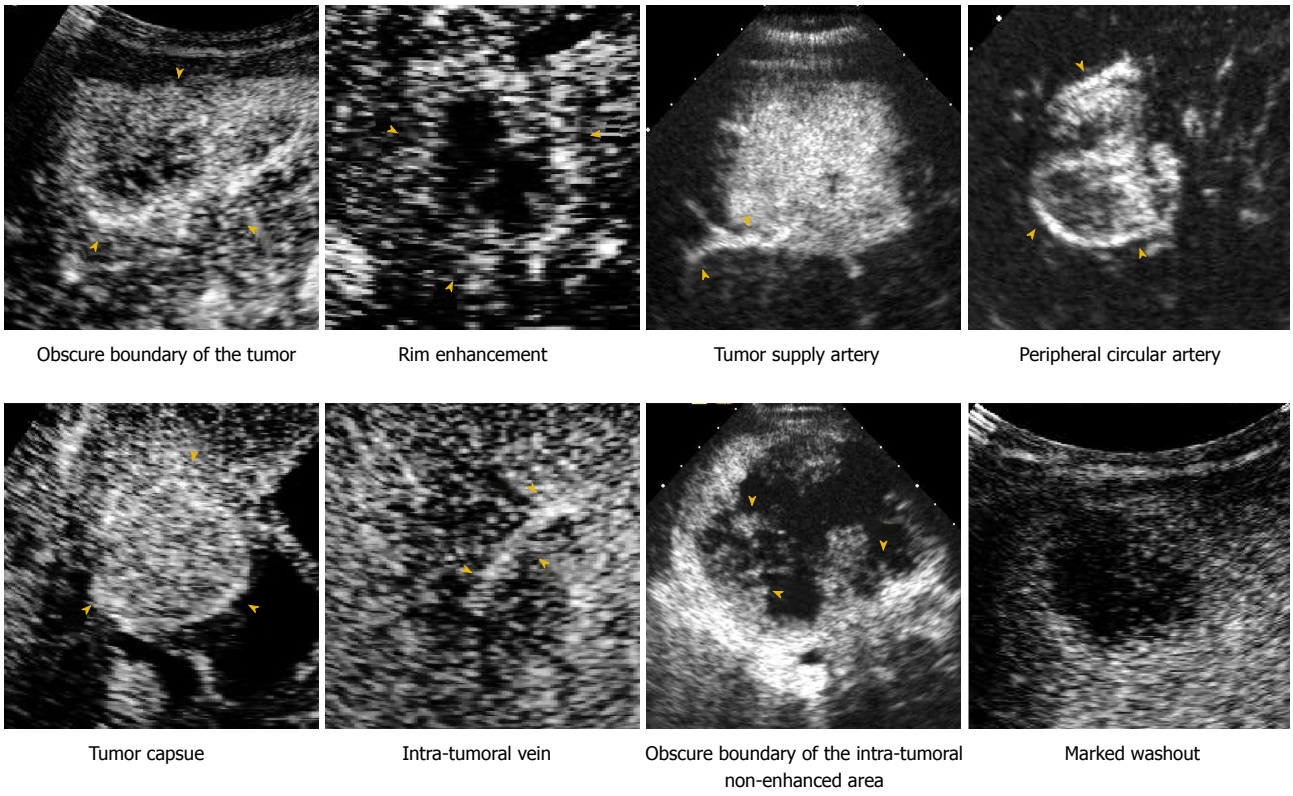

Figure 2 Contrast-enhanced ultrasound images demonstrate the enhancement features of intrahepatic cholangiocarcinoma and hepatocellular carcinoma.

dard of this study. Biopsy or surgical specimens of the hepatic lesion were fixed with 10% formalin and embedded in paraffin. The tissue slices were stained with hematoxylin-eosin. The hematoxylin-eosin slices were evaluated by a senior pathologist (Yang Z) who had more than ten years of experience with liver cancer and who was unaware of the results of any imaging or clinical examination.

Imaging techniques: The US equipment was as follows: (1) Acuson Sequoia 512 (Siemens Medical Solutions, Mountain View, CA, United States) with a 4V1 vector transducer (frequency range, 1.0-4.0 MHz) and a contrast-specific mode of contrast pulse sequencing; (2) Aplio SSA-770 or Aplio 500 (Toshiba Medical Systems, Tokyo, Japan) with a 375BT convex transducer (frequency range, 1.9-6.0 MHz) and a Contrast Harmonic Imaging mode; and (3) Aixplorer Ultrasound system (SuperSonic Imagine, Aix-en-Provence, France) equipped with the SC6-1 convex probe (frequency range, 1.0-6.0 MHz). All examinations were separately performed by three skilled radiologists (Wang W, Liang JY, Xie YX) who each had at least 15 years of experience in liver CEUS. First, the entire liver was scanned with baseline ultrasound (BUS). Then, the imaging mode was changed to CEUS, and a volume of 2.4 mL of SonoVue (Bracco, Milan, Italy) was administered. For patients with multiple nodules, only the largest lesion was selected. The target lesion was observed continuously for at least 5 min, and all imaging data were recorded. The CEUS process was classified into arterial (6-30 s after contrast agent injection), portal venous (31-120 s) and late phases (121-300 s).

Image analysis: All BUS and CEUS images were anonymized, randomized, and independently reviewed in two separate review sessions by two radiologists (Chen LD and Liang JY), who both had at least ten years of experience in liver CEUS. Neither the patient details nor the clinical or pathological results were available to them. In cases of discordance, a third investigator (Lu MD, with at least 15 years of experience in liver CEUS) reviewed the images to make the final decision. The readers were simply asked to review the enhancement appearances of the lesion instead of making a diagnosis. Therefore, the readers were informed of the fact that all patients had either ICC or HCC, but they were blinded to the final diagnosis of the target lesion.

The features on CEUS were recorded and characterized as follows (Figure 2): (1) The number of lesions; (2) maximum diameter of the target lesion; (3) shape of the target lesion; (4) boundary of the lesion; (5) enhancement level in the arterial/portal/late phase (hyper/iso-/hypo-); (6) enhancement patterns of the lesion in the arterial phase (rim/homogeneous/in homogeneous/others); (7) time to enhanced commencement; (8) washout time (within 60 s or not)[23]; (9) duration of enhancement (washout time- time to enhanced commencement); (10) tumor supply artery (defined as an artery extending from the surrounding liver parenchyma into the tumor)[24]; (11) peripheral circular artery (defined as an annular

strip artery around the tumor in the arterial phase)[24]; (12) tumor capsule (defined as an enhancement line that surrounds the tumor during the portal venous phase)[25]; (13) intratumoral vein (defined as straight vessel branches extending through the mass during the portal venous and late phase)[12,26]; (14) boundary of the intratumoral non-enhanced area (if it was present); and (15) marked washout (defined as the lesion appearing as a uniform black defect within the enhanced liver parenchyma)[23].

CEUS scoring through least absolute shrinkage and selection operator in the training set

Because of the multicollinearity of the CEUS features, we used a method of least absolute shrinkage and selection operator (LASSO)[27] regularized regression to select the most useful independent features for predicting ICC in the training set. A CEUS score was calculated for each patient via a linear combination of selected features that were weighted by their respective coefficients.

Diagnostic validation of CEUS score and comparison with CEUS LI-RADS

The constructed CEUS score was first assessed in the training set and then validated in the independent validation set and subgroups with different lesion sizes. The receiver operating characteristic (ROC) for differential diagnosis between ICC and HCC was analyzed by calculating the area under the curve (AUC) and compared with the CEUS LI-RADS. According to the CEUS LI-RADS, we classified the lesions as ICC using the definition of LR-M: rim enhancement in the arterial phase and/or early onset washout (< 60 s) and/or a marked (punched out) appearance; other lesions were defined as HCC.

Development of an individualized prediction model using the CEUS score and CEUS LI-RADS

A nomogram was developed that integrated the CEUS score and clinical information. Multivariable logistic regression analysis began with the following clinical candidate predictors: age, sex, AFP level, and CA 19-9 level. Backward stepwise selection was applied by using the likelihood ratio test with Akaike's information criterion. To provide the clinician with a quantitative tool to predict the individual probability of ICC, we built the CEUS score nomogram on the basis of multivariable logistic analysis in the training set.

With the same method, we also developed the LI-RADS nomogram after combining the CEUS LI-RADS and independent clinical predictors.

Validation of the CEUS score nomogram

The constructed predictive model was first assessed in the training set and then validated in the independent validation set. The performance of the CEUS score nomogram for predicting ICC was evaluated with respect to discrimination, calibration, and clinical usefulness and compared with the LI-RADS nomogram. The improvement in the predictive accuracy of the nomogram was evaluated by calculating the integrated discrimination improvement (IDI) and the net reclassification improvement (NRI). Subgroup analysis was also performed based on the lesion size.

Statistical analysis

Statistical analysis was performed using R software (R Foundation for Statistical Computing, version 3.2.5, http://www.r-project.org/, Austria) and Medcalc (version 11.2, Mariakerke, Belgium). Significance was set at a two-tailed $P < 0.05$. Computer-generated random numbers were used to assign 2/3 of the patients to the training dataset and 1/3 of the patients to the validation dataset. The comparison of the clinical characteristics was performed using the chi-square test and independent *t* test for continuous variables. To test the intra-observer variability of the enhancement patterns, the intraclass correlation coefficient (ICC) was calculated. The ICC was graded as follows: poor (< 0.20), moderate (0.20 to < 0.40), fair (0.40 to < 0.60), good (0.60 to < 0.80) or very good (0.80 to 1.00).

The ROC curves were plotted to demonstrate the performance of the CEUS score, LI-RADS, and nomograms in discriminating ICC from HCC in the training cohort, validation cohort and subgroups with different lesion sizes. Discrimination was quantified with the AUC. Calibration curves (*i.e.*, agreement between observed outcome frequencies and predicted probabilities) were plotted to explore the predictive accuracy of the nomograms[28]. Decision curve analysis (DCA) was conducted to determine the clinical usefulness of the nomograms by quantifying the net benefits at different threshold probabilities in the validation cohort[29].

The "*glmnet*" package of R was used for LASSO regression. The "*glm*" function was used for univariate and multivariate logistic regression analysis. The "*Hmisc*" package was used to plot the nomogram. The "*pROC*" package was used to plot the ROC curves and measure the AUC. The "*CalibrationCurves*" package was used for calibration curves. The "*DecisionCurve*" package was used to perform DCA.

RESULTS

Patients

Eighty-eight ICC and 88 HCC nodules were observed, and the study group comprised 176 nodules in 176 patients (136 men and 40 women; mean age ± SD, 55 years ± 11; range, 22-82 years) (Table 1). Hepatitis B was confirmed in 84 (95.5%) ICC patients, as well as in 86 (97.7%) HCC patients. Hepatitis B + C was confirmed in 4 (4.5%) ICC patients, as well as in 2 (2.3%) HCC patients. Alpha-fetoprotein (AFP) was elevated (> 20 μg/L) in 14 (15.9%) ICC patients and 40 (45.5%) HCC patients ($P < 0.0001$). CA19-9 was

Table 1 Demography of patients with intrahepatic cholangiocarcinoma or hepatocellular carcinoma *n* (%)

Characteristic	Training set (*n* = 117)		Validation set (*n* = 59)		*P* value
	ICC	HCC	ICC	HCC	
Number of patients	56 (47.9)	61 (52.1)	32 (27.4)	27 (23.1)	0.425
Gender					0.148
Male	35 (29.9)	56 (47.9)	24 (20.5)	21 (17.9)	
Female	21 (17.9)	5 (4.3)	8 (6.8)	6 (5.1)	
Age (yr)[1]	55 ± 11 (32-84)	55 ± 11 (32-84)	53 ± 10 (18-76)	57 ± 11 (33-82)	0.646
Hepatitis status					0.627
Hepatitis B	53 (45.3)	59 (50.4)	31 (26.5)	27 (23.1)	
Hepatitis B + C	3 (2.6)	2 (1.7)	1 (0.9)	0 (0)	
AFP > 20 (μg/L)	11 (9.4)	29 (24.8)	3 (2.6)	11 (9.4)	0.655
CA 19-9 > 35 (U/mL)	22 (18.8)	6 (5.1)	15 (12.8)	3 (2.6)	0.691
Nodule size					0.782
⩽ 3.0 cm	5 (4.3)	9 (7.7)	2 (1.7)	3 (2.6)	
3.1-5.0 cm	9 (7.7)	17 (14.5)	8 (6.8)	6 (5.1)	
> 5.0 cm	42 (35.9)	35 (29.9)	22 (18.8)	18 (15.4)	
Number of nodules					0.156
One	39 (33.3)	42 (35.9)	25 (21.4)	24 (20.5)	
Multiple	17 (14.5)	19 (16.2)	7 (6.0)	3 (2.6)	

[1]Data are means ± SD, with ranges in parentheses. Unless otherwise indicated, data are number of nodules, with percentages in parentheses. ICC: Intrahepatic cholangiocarcinoma; HCC: Hepatocellular carcinoma.

Table 2 Comparison and univariate analysis of contrast-enhanced ultrasound features between intrahepatic cholangiocarcinoma and hepatocellular carcinoma *n* (%)

CEUS features	ICC[1] (*n* = 62)	HCC[1] (*n* = 55)	*P* value	OR	(95%CI)
Irregular shape	31 (50.0)	9 (16.4)	0.000	5.037	(2.002, 13.786)
Hyper-enhanced in arterial phase	55 (88.7)	54 (98.2)	0.065	0.147	(0.003, 1.210)
Hypo/iso-enhanced in arterial phase	7 (11.3)	1 (1.8)	0.065	6.783	(0.827, 314.886)
Hypo-enhanced in portal phase	61 (98.4)	40 (72.7)	0.000	22.391	(3.206, 973.549)
Hypo-enhanced in late phase	61 (98.4)	51 (92.7)	0.186	4.728	(0.449, 239.097)
Rim-enhancement	40 (64.5)	1 (1.8)	0.000	94.271	(14.202, 3946.676)
Early washout (< 60 s)	57 (91.9)	17 (30.9)	0.000	24.563	(8.022, 92.533)
Duration of enhancement (< 30 s)	49 (79.0)	11 (20)	0.000	14.614	(5.653, 41.160)
Tumor supply artery	12 (19.4)	29 (52.7)	0.000	4.581	(1.904, 11.618)
Peripheral circular artery or tumor capsule	2 (3.2)	14 (25.5)	0.000	10.060	(2.137, 95.937)
Intra-tumoral vein	36 (58.1)	2 (3.6)	0.000	35.556	(8.118, 327.503)
Obscure boundary of tumor	43 (69.4)	12 (21.8)	0.000	7.942	(3.268, 20.550)
Obscure boundary of intra-tumoral non-enhanced area	40 (64.5)	1 (1.8)	0.000	94.271	(14.202, 3946.676)
Marked washout	38 (61.3)	1 (1.8)	0.000	82.367	(12.448, 3454.264)

[1]Data are number of cases, with percentages in parentheses. CEUS: Contrast-enhanced ultrasound; ICC: Intrahepatic cholangiocarcinoma; HCC: Hepatocellular carcinoma; OR: Odds ratio.

elevated (> 35 U/mL) in 37 (42.0%) ICC patients and 9 (10.2%) HCC patients ($P < 0.001$). No difference in any clinical characteristic was found between the training dataset and the validation dataset (all $P > 0.05$).

CEUS features distinguishing ICC from HCC

The interobserver reproducibility of the CEUS features assessment was high (Supplementary Table 1). Therefore, all results were based on the records of the first radiologist (Chen LD).

In the training set, the following features were observed more frequently in ICC than in HCC: irregular shape (31/62, 50.0%), hypo-enhancement in the portal phase (61/62, 98.4%), rim enhancement (40/62, 64.5%), early washout (< 60 s, 57/62, 91.9%), short duration of enhancement (< 30 s, 49/62, 79.0%), intratumoral vein (36/62, 58.1%), obscure boundary of tumor (43/62, 69.4%), obscure boundary of intratumoral non-enhanced area (40/62, 64.5%), and marked washout (38/62, 61.3%) (all $P < 0.05$) (Table 2).

CEUS scoring

The most useful CEUS independent variables selected by LASSO regression in the training set were as follows: rim enhancement in the arterial phase, rapid washout within 60 s, intratumoral vein, boundary of the intratumoral non-enhanced area and marked washout. Then, a CEUS score for diagnosing ICC was constructed based on the independent features as follows:

CEUS score = -1.3499017 + 1.2090675 × rim enhancement + 0.4303147 × washout within 60 s + 0.2192697 × intratumoral vein + 0.9281196 × unclear

Table 3 Comparison of the diagnostic performance of the contrast-enhanced ultrasound score *vs* contrast-enhanced ultrasound liver imaging reporting and data system in distinguishing intrahepatic cholangiocarcinoma from hepatocellular carcinoma

	Sensitivity	Specificity	PPV	NPV	Accuracy	AUC	(95%CI)	*P* value
Training set (n = 117)								
CEUS LI-RADS	0.936	0.691	0.773	0.905	0.821	0.813	(0.744, 0.882)	0.000
CEUS score	0.871	0.946	0.947	0.867	0.906	0.958	(0.924, 0.993)	
Validation set (n = 59)								
CEUS LI-RADS	1.000	0.485	0.605	1.000	0.712	0.742	(0.656, 0.829)	0.000
CEUS score	0.885	0.909	0.885	0.909	0.898	0.953	(0.907, 0.999)	
≤ 5.0 cm subgroup (n = 59)								
CEUS LI-RADS	0.917	0.600	0.611	0.913	0.729	0.758	(0.658, 0.858)	0.000
CEUS score	0.750	0.886	0.818	0.838	0.831	0.902	(0.824, 0.980)	
≤ 3.0 cm subgroup (n = 19)								
CEUS LI-RADS	0.857	0.750	0.667	0.900	0.790	0.804	(0.614, 0.993)	0.512
CEUS score	0.571	0.917	0.800	0.786	0.790	0.833	(0.636, 1.000)	

Numbers are raw data. *P* values were CEUS Score *vs* CEUS LI-RADS. CEUS: Contrast-enhanced ultrasound; LI-RADS: Liver imaging reporting and data system; ICC: Intrahepatic cholangiocarcinoma; HCC: Hepatocellular carcinoma; PPV: Positive predictive value; NPV: Negative predictive value; AUC: Area under the ROC curve.

Table 4 Univariate and multivariate logistic regression of independent variables in the prediction of intrahepatic cholangiocarcinoma

Factors	Univariate analysis		Multivariate analysis	
	OR (95%CI)	*P* value	OR (95%CI)	*P* value
Gender (female)	0.149 (0.046, 0.403)	< 0.001	0.190 (0.034,0.908)	0.044
Age (yr)				
> 40	0.786 (0.220, 2.618)	0.696	NA	NA
> 50	1.630 (0.778, 3.450)	0.197	NA	NA
AFP (mg/L) > 20	0.331 (0.148, 0.717)	0.006	0.508 (0.107, 2.212)	0.370
CA199 (U/mL) > 35	10.577 (4.152, 31.070)	< 0.001	5.352 (1.108, 30.336)	0.043
CEUS score	12.188 (5.475, 37.787)	< 0.001	14.078 (5.608, 52.831)	< 0.001

Numbers in parentheses are raw data, with 95%CI in parentheses. ICC: Intrahepatic cholangiocarcinoma; OR: Odds ratio; NA: Not available; AFP: Alpha-fetoprotein; CEUS: Contrast-enhanced ultrasound.

boundary of the intratumoral non-enhanced area + 1.1565281 × marked washout.

Diagnostic performance of the CEUS score

In the training and validation sets, the ROC analysis demonstrated that the AUCs of the CEUS score for differentiation between ICC and HCC were 0.958 and 0.953, respectively. The CEUS score showed significantly higher discriminative performance than CEUS LI-RADS (AUC = 0.742-0.813, $P < 0.001$) (Table 3).

Subgroup analysis in the validation set was also performed based on the tumor size. For tumors ≤ 5.0 cm, the AUC of the CEUS score (0.902) was much higher than that of the LI-RADS (0.758, $P < 0.001$). However, in tumors smaller than 3.0 cm, the AUC of the CEUS score was not improved compared with that of the LI-RADS ($P > 0.05$) (Table 3).

The CEUS score nomogram with clinical risk factors added

Among the clinical data, the selected independent variables for the prediction of ICC by multivariate regression analysis were sex (OR: 0.190, 95%CI: 0.034 - 0.908, $P = 0.044$) and CA 19-9 (OR: 5.352, 95%CI: 1.108-30.336, $P = 0.043$) (Table 4). Sex, CA 19-9, and the CEUS score were integrated to develop a CEUS score nomogram. A CEUS LI-RADS nomogram was also constructed integrating sex, CA 19-9, and the CEUS LI-RADS classification (Figure 3).

Discrimination of the CEUS score nomogram: The AUCs of the CEUS score nomogram in the training and validation sets were 0.971 and 0.973, respectively, which were statistically improved compared with the AUCs of the LI-RADS nomogram (AUC = 0.891-0.916, $P < 0.05$). Relative to the LI-RADS nomogram, the use of the CEUS score nomogram resulted in an NRI of 0.077 ($P = 0.488$) and an IDI of 0.152 ($P = 0.006$) in distinguishing ICC from HCC in the validation cohort (Table 5).

The results of the subanalysis in the validation set based on the tumor size demonstrated that the diagnostic performance of the CEUS score nomogram (AUC = 0.929) was far superior to that of the LI-RADS nomogram (AUC = 0.835) in differentiating a ≤ 5.0 cm ICC from HCC ($P = 0.008$). The use of the CEUS score nomogram resulted in an NRI of 0.382 ($P = 0.017$) and an IDI of 0.177 ($P = 0.002$) compared to the LI-RADS nomogram. However, in distinguishing tumors under 3 cm, the AUC, NRI, and IDI of the CEUS score

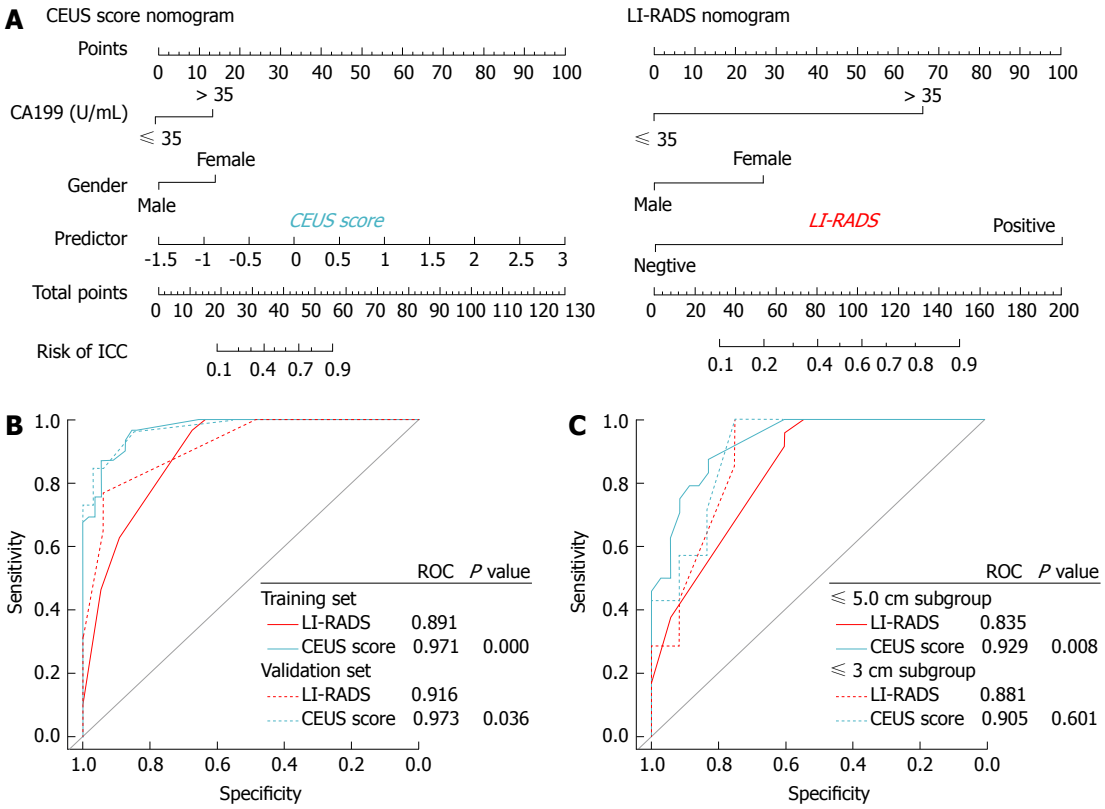

Figure 3 Contrast-enhanced ultrasound score nomogram and liver imaging reporting and data system nomogram for intrahepatic cholangiocarcinoma prediction. A: Constructed contrast-enhanced ultrasound score nomogram and liver imaging reporting and data system nomogram; B: ROC curves for the two nomograms in the training and validation set; C: ROC curves for the two nomograms in ⩽ 5.0 cm and ⩽ 3.0 cm subgroup analysis. CEUS: Contrast-enhanced ultrasound; LI-RADS: Liver imaging reporting and data system; ICC: Intrahepatic cholangiocarcinoma; HCC: Hepatocellular carcinoma.

nomogram did not show statistical improvements over the LI-RADS nomogram (all $P < 0.05$, Table 5).

Calibration for the CEUS score nomogram: The calibration plots of the CEUS score nomogram and LI-RADS nomogram applied in the validation cohort are shown in Figure 4. The CEUS score nomogram showed good agreement on the presence of ICC between the prediction and histopathological confirmation on surgical specimens. We found that the CEUS score nomogram had minimum errors (E max = 0.160) compared to the LI-RADS nomogram (E max = 0.282) in the validation set, which was consistent in tumors under ⩽ 5.0 cm (E max: 0.075 *vs* 0.119). This indicated the smallest difference in the predicted and calibrated probabilities when using the CEUS score nomogram to predict the probability of ICC. However, in distinguishing tumors under 3.0 cm, the E max of the LI-RADS nomogram (E max = 0.098) was lower than that of the CEUS score nomogram (E max = 0.121).

Clinical usefulness of the CEUS score nomogram: In both the training and validation sets, the DCA showed that the CEUS score nomogram had the highest overall net benefit compared with the LI-RADS nomogram at different threshold probabilities across the majority of the range between 0% and 95%, and the CEUS score nomogram was more beneficial than the treat-all-patients strategy or the treat-none strategy (Figure 5).

DISCUSSION

This study extends the analysis of individual specific CEUS features to a predictive model-based differential diagnosis approach. A multifeature-based CEUS diagnostic tool was identified to be an independent factor for ICC in patients at high risk of HCC in this study, with incremental value to LR-M in the LI-RADS classification. The predictive model performed better than the LR-M of the LI-RADS system in identifying ICC, which thoroughly demonstrated the incremental value of the predictive model for individualized ICC predictions in high-risk patients.

The differentiation between ICC and HCC in high-risk patients has been a challenging issue for the identification of HCC in focal liver lesions. Since the study by Vilana *et al*[5], which directed extensive attention to the diagnosis of ICC in high-risk patients, several studies have found some useful features for identifying ICC other than rim enhancement in the arterial phase. Galassi *et al*[20] found that the degree of washout intensity in the late phase was marked in 24% of ICCs ($n = 6$). Li *et al*[15,18] found that 26 out of 33 ICCs (78.8%) demonstrated both early washout (< 60 s) and marked washout in the late part of the portal phase, whereas only 6 of 50 HCCs (12.0%) showed

Table 5 Comparison of the AUC, NRI and IDI of the contrast-enhanced ultrasound score nomogram *vs* contrast-enhanced ultrasound liver imaging reporting and data system nomogram in distinguishing intrahepatic cholangiocarcinoma from hepatocellular carcinoma

	AUC	(95%CI)	*P* value	NRI	(95%CI)	*P* value	IDI	(95%CI)	*P* value
Training set (n = 117)									
CEUS LI-RADS nomogram	0.891	(0.834, 0.948)	< 0.001	0.446	(0.263, 0.629)	< 0.001	0.210	(0.140, 0.280)	< 0.001
CEUS score nomogram	0.971	(0.948, 0.995)							
Validation set (n = 59)									
CEUS LI-RADS nomogram	0.916	(0.854, 0.978)	0.036	0.077	(-0.141, 0.295)	0.488	0.152	(0.044, 0.260)	0.006
CEUS score nomogram	0.973	(0.941, 1.000)							
⩽ 5.0 cm subgroup (n = 59)									
CEUS LI-RADS nomogram	0.835	(0.744, 0.926)	0.008	0.382	(0.069, 0.695)	0.017	0.177	(0.065, 0.289)	0.002
CEUS score nomogram	0.929	(0.870, 0.988)							
⩽ 3.0 cm subgroup (n = 19)									
CEUS LI-RADS nomogram	0.881	(0.732, 1.000)	0.601	-0.202	(-0.572, 0.167)	0.283	-0.117	(-0.284, 0.050)	0.171
CEUS score nomogram	0.905	(0.772, 1.000)							

Numbers are raw data. *P* values were CEUS Score nomogram *vs* CEUS LI-RADS nomogram. AUC: Area under the ROC curve; NRI: Net reclassification improvement; IDI: Integrated discriminatory improvement; CEUS: Contrast-enhanced ultrasound; LI-RADS: Liver imaging reporting and data system; ICC: Intrahepatic cholangiocarcinoma; HCC: Hepatocellular carcinoma.

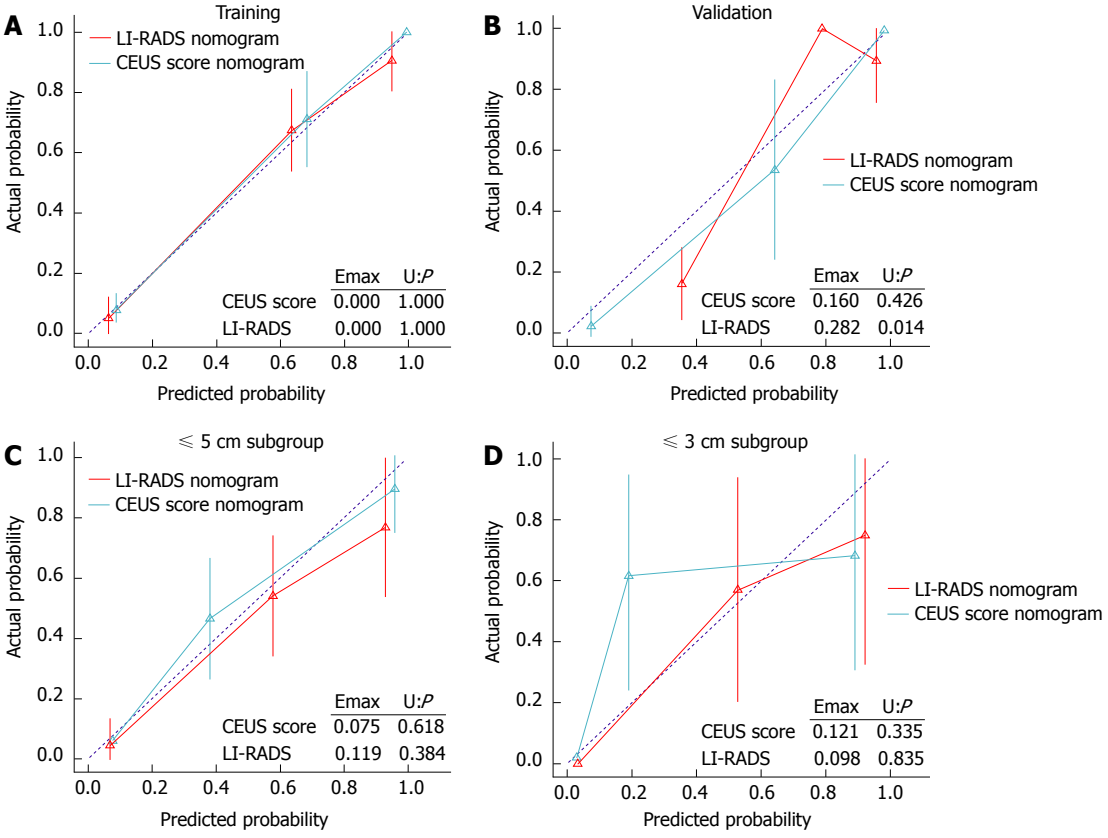

Figure 4 Calibration plots of the contrast-enhanced ultrasound score nomogram and liver imaging reporting and data system nomogram applied in the training (A), validation cohort (B), as well as ⩽ 5.0 cm (C) and ⩽ 3.0 cm subgroup (D). CEUS: Contrast-enhanced ultrasound; LI-RADS: Liver imaging reporting and data system.

these temporal enhancement features (P = 0.000). Kong *et al*[14] found that 70% of ICCs (7/10) showed more rapid washout than HCCs (P < 0.05). However, these studies depicted diverse incidence rates or sensitivities of a single feature due to small numbers of cases. The diagnostic performance and weight of these features are unknown.

To harmonize the interpretation of CEUS with that of CT and MR, the CEUS LI-RADS® system was officially released by the ACR in 2016[23]. Although the category of LR-M in the CEUS LI-RADS® represents various non-HCC malignant liver cancers, the most common malignancy aside from HCC in patients at risk for HCC is ICC[30]. As shown in our study, the sensitivity of LR-M achieved 100.0% when LR-M was used as the diagnostic criterion for ICC, which was in accordance

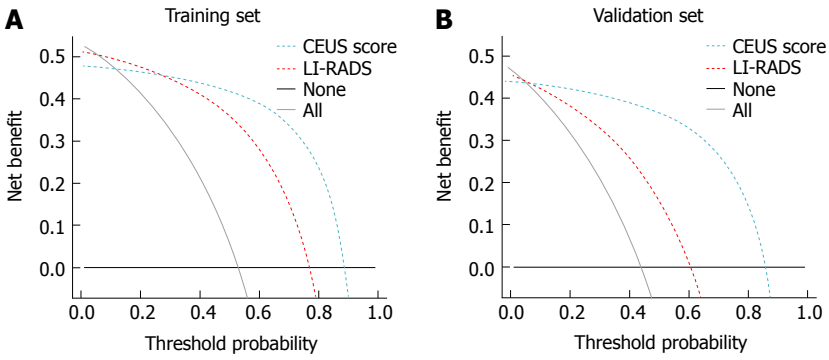

Figure 5 Decision curve analysis of the contrast-enhanced ultrasound score nomogram and liver imaging reporting and data system nomogram in the training (A) and validation cohort (B). CEUS: Contrast-enhanced ultrasound; LI-RADS: Liver imaging reporting and data system.

with the purpose of this category to preserve a high sensitivity for the detection of malignancy. However, the specificity was low (48.5%-69.1%), and that alone was insufficient for a reliable differentiation between ICC and HCC. Differentiating between ICC and HCC remains challenging. A more detailed definition of ICC might help resolve this dilemma.

In our study, we selected five specific features of ICC by LASSO regression, which is useful for addressing the collinearity between parameters. In addition to the tumor enhancement patterns of arterial phase rim enhancement, rapid washout, and marked washout proposed by the CEUS LI-RADS, we categorized two other features as tumor growth patterns and vascular invasion patterns. The boundary of the non-enhanced area in the tumor is different between ICC and HCC if the boundary is present. The non-enhanced area in ICC represents abundant fibrous tissue in the center of the tumor[31]. The border between fibrous tissue and peripheral tumor cells is obscured due to the infiltrative tumor growth of ICC, which arises from cholangiocytes[32]. However, the non-enhancing area in HCC represents necrosis, and thus, the border between necrosis and the enhanced tumor area is sharp[33]. For vascular invasion patterns, an intratumoral vessel is a characteristic of ICC. This feature is relatively frequent in CT scans[34]. Nishibori *et al*[35] have postulated that the tumor does not directly invade the portal vein but that the vein is extrinsically compressed by the tumor. On the other hand, portal vein tumor thrombosis is specific for HCC[36,37].

Another advantage of LASSO regression analysis in this study was that we could assign each feature a weight score to construct a predictive model for predicting ICC, as individualized work-up and management is often essential[38]. Since the specificity of LI-RADS was low, we integrated the above specific features to optimize the diagnostic criterion, which fully considered both sensitivity and specificity. The diagnostic performance of the CEUS score was improved compared with that of the LR-M of CEUS LI-RADS. With much higher specificity, the predictive model may have incremental value to the CEUS LI-RADS for individualized precise predictions of ICC in high-risk patients. Furthermore, we incorporated clinical risk factors into the CEUS score to construct a predictive model, which may be more applicable in clinical practice. The discriminative performance of the CEUS score nomogram was also better than that of the LI-RADS nomogram.

We performed subgroup analysis according to the tumor size and found that the CEUS score significantly improved the discriminative performance in the $\leqslant$ 5.0 cm subgroup compared to the LI-RADS. However, the discriminative performance did not improve in the $\leqslant$ 3.0 cm subgroup. This may be because small ICCs lack specific enhancement characteristics selected by LASSO regression. Since the NRI and IDI were decreased in the $\leqslant$ 3.0 cm lesions, the LI-RADS nomogram was superior to the CEUS score nomogram for small lesions, while the CEUS score nomogram was recommended for lesions larger than 3.0 cm.

Our study has several limitations. First, we did not enroll all focal liver lesions to validate the diagnostic accuracy of the CEUS LI-RADS. The main purpose of this study was to refine the CEUS diagnostic algorithm for ICC in high-risk patients, so we only selected patients with ICC or HCC. The readers did not know the purpose of the study and were only asked to record CEUS features. Therefore, the design and process of this study are reasonable. Second, this is a retrospective study. Prospective studies are mandatory in our future work. Third, the study focused on high-risk patients with chronic hepatitis B or hepatitis C or cirrhosis. As a result, only 88 high-risk patients with ICC were evaluable for the purpose of the study, and this decreased the strength of the study. Fourth, specimens from liver biopsy or surgery and selection of HCC group could affect the present result. Fifth, we analyzed the records on radiologist. This will increase the subjectivity of the study. Finally, we did not compare the diagnostic performance of CEUS with that of MRI/CT. Because of the large number of patients in our hospital, the delay phase scanning of MRI/CT was not performed routinely for each patient with a liver lesion. As a result,

the comparison was not achieved due to the missing information of the delay phase, which was crucial for the differentiation of ICC and HCC by MRI/CT. This is a relevant limitation of the study given that MRI/CT scans must be performed in clinical practice according to international guidelines.

In conclusion, we developed a CEUS predictive model for predicting ICC in high-risk patients with improved discriminative accuracy compared to the LR-M of the CEUS LI-RADS in tumors larger than 3.0 cm. This tool may serve as a useful supplement to the CEUS LI-RADS and further improve the diagnostic efficiency of CEUS. For small tumors, the CEUS LI-RADS is recommended. A large prospective trial is necessary to confirm the conclusion.

ARTICLE HIGHLIGHTS

Research background

Intrahepatic cholangiocarcinoma (ICC) is a highly malignant epithelial cancer originating from bile ducts with cholangiocyte differentiation. In recent years, chronic cirrhosis and viral hepatitis have been recognized as important risk factors for ICC development. ICC has been increasingly found in patients with cirrhosis, and distinguishing between ICC and hepatocellular carcinoma (HCC) is a major clinical issue because the management and prognosis of these conditions differ significantly.

Research motivation

The contrast-enhanced ultrasound (CEUS) Liver Imaging Reporting and Data System (LI-RADS®) sets the specific category of LR-M for distinguishing ICC from HCC, but the diagnostic dilemma remains unresolved. Additionally, no study has validated the performance of LR-M as the differential diagnostic criterion for ICC and HCC.

Research objectives

To identify important imaging predictors of ICC on CEUS, to develop a novel diagnostic nomogram incorporating clinical, CEUS and laboratory characteristics that could be used to accurately predict the risk of ICC in high-risk patients and to compare the nomogram with modified CEUS LI-RADS.

Research methods

This retrospective study consisted of 88 consecutive high-risk patients with ICC and 88 high-risk patients with HCC selected by propensity score matching between May 2004 and July 2016. Patients were assigned to two groups, namely, a training set and validation set, at a 1:1 ratio. A CEUS score for diagnosing ICC was generated based on significant CEUS features. Then, a nomogram based on the CEUS score was developed, integrating the clinical data. The performance of the nomogram was then validated and compared with that of the LR-M of the CEUS LI-RADS.

Research results

The most useful CEUS features for ICC were as follows: rim enhancement (64.5%), early washout (91.9%), intratumoral vein (58.1%), obscure boundary of intratumoral non-enhanced area (64.5%), and marked washout (61.3%, all $P < 0.05$). In the validation set, the area under the curve (AUC) of the CEUS score (AUC = 0.953) for differentiation between ICC and HCC were improved compared to the LI-RADS (AUC = 0.742) ($P < 0.001$). When clinical data were added, the CEUS score nomogram was superior to the LI-RADS nomogram (AUC: 0.973 *vs* 0.916, $P = 0.036$, NRI: 0.077, IDI: 0.152). Subgroup analysis demonstrated that the CEUS score model was notably improved compared to the LI-RADS in under 5.0 cm tumors ($P < 0.05$) but not improved in tumors under 3.0 cm ($P > 0.05$).

Research conclusions

A CEUS score for predicting ICC consisted of more detailed CEUS features (rim enhancement, early washout, intratumoral vein, obscure boundary of intratumoral non-enhanced area, and marked washout) was constructed.

The diagnostic performance of the CEUS score (AUC = 0.953) for differentiation between ICC and HCC was improved compared to the LR-M of LI-RADS (AUC = 0.742) ($P < 0.001$). A CEUS score nomogram that added the clinical risk factors was superior to the LI-RADS nomogram (AUC: 0.973 *vs* 0.916, $P = 0.036$, NRI: 0.077, IDI: 0.152). The CEUS score predictive model was notably improved compared to the LI-RADS in ≤ 5.0 cm tumors ($P < 0.05$) but not improved in tumors ≤ 3.0 cm ($P > 0.05$).

Research perspectives

The CEUS predictive model for differentiation between ICC and HCC in high-risk patients had improved discrimination and clinical usefulness compared to the CEUS LI-RADS.

REFERENCES

1 **Lim JH.** Cholangiocarcinoma: morphologic classification according to growth pattern and imaging findings. *AJR Am J Roentgenol* 2003; **181**: 819-827 [PMID: 12933488 DOI: 10.2214/ajr.181.3.1810819]

2 **Khan SA**, Thomas HC, Davidson BR, Taylor-Robinson SD. Cholangiocarcinoma. *Lancet* 2005; **366**: 1303-1314 [PMID: 16214602 DOI: 10.1016/S0140-6736(05)67530-7]

3 **Blechacz B**, Gores GJ. Cholangiocarcinoma: advances in pathogenesis, diagnosis, and treatment. *Hepatology* 2008; **48**: 308-321 [PMID: 18536057 DOI: 10.1002/hep.22310]

4 **Kim SJ**, Lee JM, Han JK, Kim KH, Lee JY, Choi BI. Peripheral mass-forming cholangiocarcinoma in cirrhotic liver. *AJR Am J Roentgenol* 2007; **189**: 1428-1434 [PMID: 18029881 DOI: 10.2214/AJR.07.2484]

5 **Vilana R**, Forner A, Bianchi L, García-Criado A, Rimola J, de Lope CR, Reig M, Ayuso C, Brú C, Bruix J. Intrahepatic peripheral cholangiocarcinoma in cirrhosis patients may display a vascular pattern similar to hepatocellular carcinoma on contrast-enhanced ultrasound. *Hepatology* 2010; **51**: 2020-2029 [PMID: 20512990 DOI: 10.1002/hep.23600]

6 **Bruix J**, Sherman M; American Association for the Study of Liver Diseases. Management of hepatocellular carcinoma: an update. *Hepatology* 2011; **53**: 1020-1022 [PMID: 21374666 DOI: 10.1002/hep.24199]

7 **Omata M**, Lesmana LA, Tateishi R, Chen PJ, Lin SM, Yoshida H, Kudo M, Lee JM, Choi BI, Poon RT, Shiina S, Cheng AL, Jia JD, Obi S, Han KH, Jafri W, Chow P, Lim SG, Chawla YK, Budihusodo U, Gani RA, Lesmana CR, Putranto TA, Liaw YF, Sarin SK. Asian Pacific Association for the Study of the Liver consensus recommendations on hepatocellular carcinoma. *Hepatol Int* 2010; **4**: 439-474 [PMID: 20827404 DOI: 10.1007/s12072-010-9165-7]

8 **Dietrich CF**, Cui XW, Boozari B, Hocke M, Ignee A. Contrast-enhanced ultrasound (CEUS) in the diagnostic algorithm of hepatocellular and cholangiocellular carcinoma, comments on the AASLD guidelines. *Ultraschall Med* 2012; **33** Suppl 1: S57-S66 [PMID: 22723030 DOI: 10.1055/s-0032-1312903]

9 **Barreiros AP**, Piscaglia F, Dietrich CF. Contrast enhanced ultrasound for the diagnosis of hepatocellular carcinoma (HCC): comments on AASLD guidelines. *J Hepatol* 2012; **57**: 930-932 [PMID: 22739095 DOI: 10.1016/j.jhep.2012.04.018]

10 **Quaia E**, Lorusso A, Grisi G, Stacul F, Cova MA. The role of CEUS in the characterization of hepatocellular nodules detected during the US surveillance program--current practices in Europe. *Ultraschall Med* 2012; **33** Suppl 1: S48-S56 [PMID: 22723029 DOI: 10.1055/s-0032-1312899]

11 **Bohle W**, Clemens PU, Heubach T, Zoller WG. Contrast-enhanced ultrasound (CEUS) for differentiating between hepatocellular

and cholangiocellular carcinoma. *Ultraschall Med* 2012; **33**: E191-E195 [PMID: 22194045 DOI: 10.1055/s-0031-1282029]
12 **Chen LD**, Xu HX, Xie XY, Xie XH, Xu ZF, Liu GJ, Wang Z, Lin MX, Lu MD. Intrahepatic cholangiocarcinoma and hepatocellular carcinoma: differential diagnosis with contrast-enhanced ultrasound. *Eur Radiol* 2010; **20**: 743-753 [PMID: 19760416 DOI: 10.1007/s00330-009-1599-8]
13 **Han J**, Liu Y, Han F, Li Q, Yan C, Zheng W, Wang J, Guo Z, Wang J, Li A, Zhou J. The Degree of Contrast Washout on Contrast-Enhanced Ultrasound in Distinguishing Intrahepatic Cholangiocarcinoma from Hepatocellular Carcinoma. *Ultrasound Med Biol* 2015; **41**: 3088-3095 [PMID: 26386477 DOI: 10.1016/j.ultrasmedbio.2015.08.001]
14 **Kong WT**, Wang WP, Huang BJ, Ding H, Mao F. Value of wash-in and wash-out time in the diagnosis between hepatocellular carcinoma and other hepatic nodules with similar vascular pattern on contrast-enhanced ultrasound. *J Gastroenterol Hepatol* 2014; **29**: 576-580 [PMID: 24118042 DOI: 10.1111/jgh.12394]
15 **Li R**, Yuan MX, Ma KS, Li XW, Tang CL, Zhang XH, Guo DY, Yan XC. Detailed analysis of temporal features on contrast enhanced ultrasound may help differentiate intrahepatic cholangiocarcinoma from hepatocellular carcinoma in cirrhosis. *PLoS One* 2014; **9**: e98612 [PMID: 24874413 DOI: 10.1371/journal.pone.0098612]
16 **Liu GJ**, Wang W, Lu MD, Xie XY, Xu HX, Xu ZF, Chen LD, Wang Z, Liang JY, Huang Y, Li W, Liu JY. Contrast-Enhanced Ultrasound for the Characterization of Hepatocellular Carcinoma and Intrahepatic Cholangiocarcinoma. *Liver Cancer* 2015; **4**: 241-252 [PMID: 26779444 DOI: 10.1159/000367738]
17 **Wildner D**, Bernatik T, Greis C, Seitz K, Neurath MF, Strobel D. CEUS in hepatocellular carcinoma and intrahepatic cholangiocellular carcinoma in 320 patients - early or late washout matters: a subanalysis of the DEGUM multicenter trial. *Ultraschall Med* 2015; **36**: 132-139 [PMID: 25812115 DOI: 10.1055/s-0034-1399147]
18 **Li R**, Zhang X, Ma KS, Li XW, Xia F, Zhong H, Tang CL, Guo Y, Yan XC. Dynamic enhancing vascular pattern of intrahepatic peripheral cholangiocarcinoma on contrast-enhanced ultrasound: the influence of chronic hepatitis and cirrhosis. *Abdom Imaging*2013; **38**: 112-119 [PMID: 22323003 DOI: 10.1007/s00261-012-9854-x]
19 **Lu Q**, Xue LY, Wang WP, Huang BJ, Li CX. Dynamic enhancement pattern of intrahepatic cholangiocarcinoma on contrast-enhanced ultrasound: the correlation with cirrhosis and tumor size. *Abdom Imaging* 2015; **40**: 1558-1566 [PMID: 25725793 DOI: 10.1007/s00261-015-0379-y]
20 **Galassi M**, Iavarone M, Rossi S, Bota S, Vavassori S, Rosa L, Leoni S, Venerandi L, Marinelli S, Sangiovanni A, Veronese L, Fraquelli M, Granito A, Golfieri R, Colombo M, Bolondi L, Piscaglia F. Patterns of appearance and risk of misdiagnosis of intrahepatic cholangiocarcinoma in cirrhosis at contrast enhanced ultrasound. *Liver Int* 2013; **33**: 771-779 [PMID: 23445369 DOI: 10.1111/liv.12124]
21 **Stroffolini T**, Gaeta GB, Mele A. AASLD Practice Guidelines on chronic hepatitis B and HBV infection in Italy. *Hepatology* 2007; **46**: 608-609; author reply 609 [PMID: 17661422 DOI: 10.1002/hep.21841]
22 **Baek S**, Park SH, Won E, Park YR, Kim HJ. Propensity score matching: a conceptual review for radiology researchers. *Korean J Radiol* 2015; **16**: 286-296 [PMID: 25741190 DOI: 10.3348/kjr.2015.16.2.286]
23 **Piscaglia F**, Wilson SR, Lyshchik A, Cosgrove D, Dietrich CF, Jang HJ, Kim TK, Salvatore V, Willmann JK, Sirlin CB, Kono Y. American College of Radiology Contrast Enhanced Ultrasound Liver Imaging Reporting and Data System (CEUS LI-RADS) for the diagnosis of Hepatocellular Carcinoma: a pictorial essay. *Ultraschall Med* 2017; **38**: 320-324 [PMID: 28329875 DOI: 10.1055/s-0042-124661]
24 **Catalano O**, Nunziata A, Lobianco R, Siani A. Real-time harmonic contrast material-specific US of focal liver lesions. *Radiographics* 2005; **25**: 333-349 [PMID: 15798053 DOI: 10.1148/rg.252045066]
25 **Schellhaas B**, Görtz RS, Pfeifer L, Kielisch C, Neurath MF, Strobel D. Diagnostic accuracy of contrast-enhanced ultrasound for the differential diagnosis of hepatocellular carcinoma: ESCULAP versus CEUS-LI-RADS. *Eur J Gastroenterol Hepatol* 2017; **29**: 1036-1044 [PMID: 28562394 DOI: 10.1097/MEG.0000000000000916]
26 **Xu HX**, Lu MD, Liu GJ, Xie XY, Xu ZF, Zheng YL, Liang JY. Imaging of peripheral cholangiocarcinoma with low-mechanical index contrast-enhanced sonography and SonoVue: initial experience. *J Ultrasound Med* 2006; **25**: 23-33 [PMID: 16371552 DOI: 10.7863/jum.2006.25.1.23]
27 **Zhang JX**, Song W, Chen ZH, Wei JH, Liao YJ, Lei J, Hu M, Chen GZ, Liao B, Lu J, Zhao HW, Chen W, He YL, Wang HY, Xie D, Luo JH. Prognostic and predictive value of a microRNA signature in stage II colon cancer: a microRNA expression analysis. *Lancet Oncol* 2013; **14**: 1295-1306 [PMID: 24239208 DOI: 10.1016/S1470-2045(13)70491-1]
28 **Coutant C**, Olivier C, Lambaudie E, Fondrinier E, Marchal F, Guillemin F, Seince N, Thomas V, Levêque J, Barranger E, Darai E, Uzan S, Houvenaeghel G, Rouzier R. Comparison of models to predict nonsentinel lymph node status in breast cancer patients with metastatic sentinel lymph nodes: a prospective multicenter study. *J Clin Oncol* 2009; **27**: 2800-2808 [PMID: 19349546 DOI: 10.1200/JCO.2008.19.7418]
29 **Vickers AJ**, Cronin AM, Elkin EB, Gonen M. Extensions to decision curve analysis, a novel method for evaluating diagnostic tests, prediction models and molecular markers. *BMC Med Inform Decis Mak* 2008; **8**: 53 [PMID: 19036144 DOI: 10.1186/1472-6947-8-53]
30 **Joo I**, Lee JM, Lee SM, Lee JS, Park JY, Han JK. Diagnostic accuracy of liver imaging reporting and data system (LI-RADS) v2014 for intrahepatic mass-forming cholangiocarcinomas in patients with chronic liver disease on gadoxetic acid-enhanced MRI. *J Magn Reson Imaging* 2016; **44**: 1330-1338 [PMID: 27087012 DOI: 10.1002/jmri.25287]
31 **Xu HX**, Chen LD, Liu LN, Zhang YF, Guo LH, Liu C. Contrast-enhanced ultrasound of intrahepatic cholangiocarcinoma: correlation with pathological examination. *Br J Radiol* 2012; **85**: 1029-1037 [PMID: 22374276 DOI: 10.1259/bjr/21653786]
32 **Bridgewater J**, Galle PR, Khan SA, Llovet JM, Park JW, Patel T, Pawlik TM, Gores GJ. Guidelines for the diagnosis and management of intrahepatic cholangiocarcinoma. *J Hepatol* 2014; **60**: 1268-1289 [PMID: 24681130 DOI: 10.1016/j.jhep.2014.01.021]
33 **Ogawa S**, Kumada T, Toyoda H, Ichikawa H, Kawachi T, Otobe K, Hibi T, Takeshima K, Kiriyama S, Sone Y, Tanikawa M, Hisanaga Y, Yamaguchi A, Isogai M, Kaneoka Y, Washizu J. Evaluation of pathological features of hepatocellular carcinoma by contrast-enhanced ultrasonography: comparison with pathology on resected specimen. *Eur J Radiol* 2006; **59**: 74-81 [PMID: 16545532 DOI: 10.1016/j.ejrad.2006.02.003]
34 **Han JK**, Choi BI, Kim AY, An SK, Lee JW, Kim TK, Kim SW. Cholangiocarcinoma: pictorial essay of CT and cholangiographic findings. *Radiographics* 2002; **22**: 173-187 [PMID: 11796906 DOI: 10.1148/radiographics.22.1.g02ja15173]
35 **Nishibori H**, Kanematsu M, Hoshi H, Kondo H, Yamawaki Y, Kawaguchi Y, Kato M, Yamada T. Small peripheral cholangiocarcinoma with undisturbed transiting portal vein: radiologic-pathologic correlation. *AJR Am J Roentgenol* 1999; **173**: 1243-1245 [PMID: 10541096 DOI: 10.2214/ajr.173.5.10541096]
36 **Tarantino L**, Francica G, Sordelli I, Esposito F, Giorgio A, Sorrentino P, de Stefano G, Di Sarno A, Ferraioli G, Sperlongano P. Diagnosis of benign and malignant portal vein thrombosis in cirrhotic patients with hepatocellular carcinoma: color Doppler US, contrast-enhanced US, and fine-needle biopsy. *Abdom Imaging* 2006; **31**: 537-544 [PMID: 16865315 DOI: 10.1007/s00261-005-0150-x]
37 **Sparchez Z**, Radu P, Zaharia T, Kacso G, Diaconu B, Grigorescu

I, Badea R. B-mode and contrast enhanced ultrasound guided biopsy of portal vein thrombosis. Value in the diagnosis of occult hepatocellular carcinoma in liver cirrhosis. *Med Ultrason* 2010; **12**: 286-294 [PMID: 21210013]

38 **An C**, Kim DW, Park YN, Chung YE, Rhee H, Kim MJ. Single Hepatocellular Carcinoma: Preoperative MR Imaging to Predict Early Recurrence after Curative Resection. *Radiology* 2015; **276**: 433-443 [PMID: 25751229 DOI: 10.1148/radiol.15142394]

P- Reviewer: Kao JT, Rimassa L, Xu LB **S- Editor**: Gong ZM
L- Editor: Filipodia **E- Editor**: Bian YN

Published by **Baishideng Publishing Group Inc**
7901 Stoneridge Drive, Suite 501, Pleasanton, CA 94588, USA
Telephone: +1-925-223-8242
Fax: +1-925-223-8243
E-mail: bpgoffice@wjgnet.com
Help Desk: http://www.f6publishing.com/helpdesk
http://www.wjgnet.com

ISSN 1007-9327